heritage

MDPI

Article

Analysing Objects to Tailor Environmental Preventive Conservation

David Thickett [1,*], Nicola Emmerson [2], Rene Larsen [3], Marianne Odlyha [4] and David Watkinson [2]

[1] English Heritage Trust, London SE10 8QX, UK
[2] School of History, Archaeology and Religion, University of Cardiff, Cardiff CF10 3AT, UK
[3] Conservation Zealand-Knowledge Centre for the Preservation of Cultural Heritage, 4600 Køge, Denmark
[4] Department of Biological Sciences Birkbeck, University of London, London WC1E 7HX, UK
* Correspondence: david.thickett@english-heritage.org.uk; Tel.: +44-7770397964

Abstract: This work explores the potential of analyzing individual objects to improve their preventive conservation. Previously, environmental recommendations have been based on an average or worst response of material groups. Cultural heritage objects are extremely variable and within a group such as archaeological iron a very wide range of responses are shown. Characterizing a single object's response allows its environment to be tailored to its requirements and can enable significant resource and carbon footprint savings. Three main approaches are considered with a material explored in detail including preventive conservation ramifications. Composition analysis is investigated through the stability of limestones. The critical concentrations of soluble salts causing surface deterioration in one environment has been explored. A more rapid method of analyzing clays in acid insoluble fractions from drillings and undertaking that analysis non-invasively has been developed. Measuring deterioration rates is explored through oxygen consumption analyses of archaeological iron. The distributions of previously published data are explored and the changes in rates examined. A scheme for parchment based on shrinkage temperatures and observations is presented for the first time and its use illustrated with a newly acquired letter. The type of work required to produce these schemes is explored with leather.

Keywords: soluble salts; clays; oxygen depletion; shrinkage temperature; leather; parchment; limestone

Citation: Thickett, D.; Emmerson, N.; Larsen, R.; Odlyha, M.; Watkinson, D. Analysing Objects to Tailor Environmental Preventive Conservation. *Heritage* **2023**, *6*, 212–235. https://doi.org/10.3390/heritage6010011

Academic Editor: Alessandra Bonazza

Received: 12 October 2022
Revised: 2 December 2022
Accepted: 21 December 2022
Published: 26 December 2022

1. Introduction

Materials science effectively dictates the value of preventive conservation, since its outcomes define criteria applied by practitioners. Conservation and care of collections increasingly uses specified values and ranges for variables, such as relative humidity (RH), temperature and light, to delineate safe criteria for storage and display of materials, as well as for identifying regions of risk. These values form the preventive conservation evidence that is used to argue for resources and design specifications within the heritage sector. Their value in practice is related to the strength of the data used to derive them. Understanding structure and decay mechanisms and rate of change are essential factors for deriving preservation standards. This paper focuses on the individuality of objects and what this may mean for setting standards.

Preventive conservation has treated cultural heritage objects by material groups, thought to react to the environment in similar ways [1,2]. Whilst it has long been understood that some similar materials can react very differently [3–9], only recently has sufficient research been completed to predict and understand this reactivity and use it to tailor environmental controls. Understanding the reactivity of a single object overcomes the broad classes defined by material types and can remove some of the uncertainty from behaviour prediction. This approach has significant potential to stretch limited resources and improve sustainability of environmental preventive conservation. Three different analytical approaches have been used to date for understanding a single object:

- Analysing its composition.
- Measuring its deterioration rate.
- Examining its state of preservation or evidence of degradation markers.

Collectively, the data derived from material composition, deterioration rate and preservation state must be balanced and, where possible, integrated to offer the best insight into controlling change of materials. This is a challenging goal, as numerical data that is readily extrapolated forwards to predict future change is the ideal outcome, yet it is exceptionally difficult to achieve predictably. This paper reports a range of datasets which explore these three analytical approaches, accompanied by discussion of their context in relation to this goal, which aims to illustrate the complexity of deriving such data. The use of individual object data helps with the potential problems of using defined environmental standards in a universal manner. Each approach is illustrated by an example application to a particular object type. For state of preservation, two examples are given, one for parchment based on an existing scheme and a second for leather which illustrates the intial processes in developing a scheme. The examples are illustrative and were selected for instances where sufficient information exists. The impact of the environment on the deterioration of most materials has not been studied in sufficient detail to apply this approach.

2. Analysing the Composition of an Object

Material composition can significantly influence reaction rates within an environment. This reactivity can be a function of natural composition, impurities introduced into a material, or manufacturing components. For example, the purity of lead [6], and trace concentrations of arsenic and cadmium [7], are reported to affect its corrosion rate significantly when acetic acid is present. Weeping glass is much more sensitive towards relative humidity than most glass, with its sensitivity being driven by silica concentration, sodium and potassium content and stabiliser (calcium, barium, lead) concentrations [5,8]. The deterioration of paper has been attributed to 90% manufacture (composition) and 10% environment [9]. To explore how analysing the composition of an object can contribute to its conservation management, the example of limestone artefacts in the British Museum is considered.

2.1. Analysing Limestone Composition: Introduction

The presence of soluble salt contaminants (analysed by drilling, water extraction and specific ion electrodes or ion chromatography) and expanding clays in the acid insoluble fraction of limestones (analysed by drilling, acid digestion and X-ray diffraction) has been linked with deterioration [10,11]. For Egyptian limestones in the British Museum, the relationship has been tested statistically within that environment in a previously published study [10]. Objects with higher nitrate concentrations (all objects had chloride but no sulfate present) were observed to have decayed and those with expanding clay contents above 5% suffered both structural and surface decay [10] but this empirical relationship is only valid for the environment prevailing within the rooms in the British Museum holding these objects. Further analyses of salt concentrations and assessment of when they lead to visible surface damage have since been undertaken and are reported here.

Thermodynamic modelling can be used to determine relative humidity/temperature fields under which the identified salts present will generate high pressures which could damage the substrate [12–16] but this model is reported to be uncertain for nitrates due to the sparsity of available solubility data. Experiments testing the ECOS predictions for chloride/nitrate salt laden Caen stone pieces, supported by observations of damage in display environments, are reported here. Both near infra-red and FTIR spectroscopies are examined as rapid methods for the analysis of clays in acid digested samples. The common X-ray diffraction technique relies on producing an aligned sample to show clearly the basal plane reflections on which identification is based [17]. However, the RH responsive nature of the clays of interest means that they frequently curl off the filter when drying, making them unsuitable for XRD analysis. The possibility of employing non-invasive methods to

analyse and quantify clays present in limestones, without the need to drill samples, was also investigated. Examination of limestone cross sections has indicated some bedding of clays running parallel to surfaces. To address this potential analytical limitation, the depth from which clays could be analysed under calcite with FTIR and NIR was also investigated.

2.2. Analysing Limestone Composition: Method

Samples of Egyptian limestones from the British Museum collections and a medieval British sculpture, 'Christ in Majesty' were analysed. Caen stone specimens were utilised for both tests in an environmental chamber and in situ.

To identify the salts present in Egyptian limestones, a series of small drillings into break surfaces were taken using a 3 mm drill bit. Powder from the first 1 mm drilling was collected then the powder was incrementally collected to 22 mm depth. The powder samples were dried at 110 °C until no further mass loss occurred. Samples of the dry powders (0.1 g) were extracted with 10 mL of 18.2 MΩ/cm water, filtered and analysed with a Dionex 600 ion chromatograph. This used AS14 columns with 8 mM sodium carbonate, 18 mM sodium bicarbonate eluent for anions and CS12 column with 1 mM methane sulfonic acid eluent for cations. The analysed salt concentrations were fed into the ECOS model (RUNSALT version 1.9) to determine the RH regions generating solid products at 20 °C. This was the temperature mode of the rooms used to house the limestone sculptures analysed.

Caen stone has been used as an experimental substrate to mimic Egyptian limestones due to its fine-grained nature and similar pore size distribution [18]. Deteriorated Egyptian limestone was found to have over 32% of its pore volume with pore sizes less than 0.1 μm [10] and the Caen stone samples used had over 28%. To investigate physical damage caused by salts, small Caen stone cubes (50 g) were impregnated with salt mixtures (sodium chloride and nitrate) as detailed in Table 1, to replicate those found in the limestone objects (detailed in Figure 1). After drying, (at 40% RH for chamber tests and 45% RH for room tests to match likely room RH conditions), any salts on the surface were removed by brushing, and the percentage salt impregnated was estimated from the mass increase of the dried stone after impregnation.

Table 1. Salt concentrations in impregnated Caen stone blocks.

Sample Number	Dried Percentage Salt	Impregnation Solution $NaCl/NaNO_3$ (Nitrate to Chloride Ratio)
1	0.4	1:1
2	2.3	1:1
3	0.4	1:2
4	2.3	1:2
5	0.4	1:3
6	2.3	1:3

The salt impregnated blocks were placed on Melinex sheets in a Sanyo environmental chamber and subjected to 10 cycles of 40 to 70 to 40% RH, with 48 h at each RH value, at 20 °C. This cycle was based on environmental monitoring from the three locations in the British Museum where most Egyptian limestone sculpture is displayed or stored. The mass of the blocks was recorded on an AND EK200 balance in the chamber. The balance was placed on 4 circular Sorbothane blocks to attenuate vibrations at 13 Hz due to the fan used in the chamber. The dominant frequency was determined using a RDP298 shocklog and the mass of balance and sample matched to that of the shocklog. The thickness and size of the circles was determined using the design guide calculator version 2, published by Sorbothane. After the cycling, any salts present on the surfaces of the blocks were brushed off, collected and added to any salts on the Melinex. These were dried and their soluble anion content analysed by water extraction and ion chromatography, as previously

reported. The presence of any calcite in the salt was determined by pressing 3 mg of the dried extracted powder into a 300 mg KBr disc and analysing with FTIR (Nicolet 510PC) with a suitable calibration for the 711 cm^{-1} peak.

Figure 1. Objects discussed including Christ in Majesty sculpture.

Two other sets of salt impregnated blocks were placed on Melinex sheets on display furniture in the Egyptian Sculpture Gallery and subsequently in a store room, both at the British Museum. They were in situ for a total of 3 years between the two locations. Only the higher salt content blocks 2, 4 and 6 were exposed, as the number of relative humidity cycles was expected to be much lower than with the environmental chamber exposure. Any salts on the surfaces were brushed off and collected every 6 months. Any losses of material onto the Melinex were collected separately, with soluble salts and calcite analysed as before.

Samples of clays procured commercially, or from acid digestion of limestones, were analysed with a Bruker Alpha FTIR with ATR accessory or Analytic Labspec 4 NIR spectrometer. To investigate non-invasive analyses, powders were then mixed with calcite powder to produce mixtures from 1 to 15% of the clay by mass. The mixtures were analysed with Bruker Alpha FTIR with direct reflectance accessory and Analytic Labspec 4 NIR spectrometer. Once the method had been developed, it was applied to 100 limestone sculpture objects. To investigate the information depth of the analyses, calcite (Analar BDH) powder was pressed into a series of discs of different thickness from 0.5 to 4 mm using a KBr pellet press. The FTIR analyses of the clay and calcite mixtures were then repeated with the calcite discs of different thicknesses inserted between the mixed clay sample and the spectrometer, and the calcite depth from which an analysis can be made was determined.

The limestone sculpture of Christ in Majesty from Fountains Abbey in English Heritage's collection was showing rapid structural decay with salt crystals observed on the surfaces. No further analysis of the limestone type had been undertaken. The storage environment was similar in RH to that of the main rooms used for Egyptian limestone. A drilling, as described previously, was taken from one of the numerous break surfaces. The soluble salt and acid insoluble contents were analysed as above.

2.3. Analysing Limestone Composition: Results and Discussion

The salts analyses from Egyptian limestones are shown in Figure 2. Over 99.5% of the cations detected were sodium in all instances.

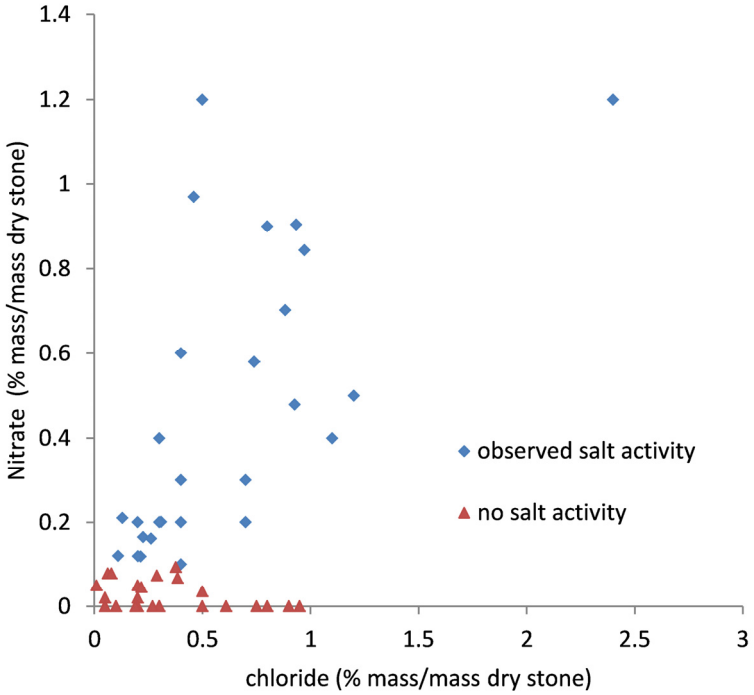

Figure 2. Chloride and nitrate salt contents in Egyptian limestone sculpture.

There is a clear boundary at around 0.1% mass/mass dry stone for nitrate. Stones above this concentration showed signs of salt surface damage, with powdering or small pieces lifting. The chloride concentrations overlapped significantly between 0 and 0.5%, although several of the objects observed to be deteriorating had much higher concentrations. The results extend the work reported in Bradley and Middleton [10] beyond the structural decay investigated. Although less dramatic than the structural decay reported previously, any surface loss reduces the heritage value of sculpture. Predominantly sodium was detected as a cation, over 99.5% in all instances.

Table 2 shows the deterioration observed in environmental chamber tests.

Table 2. Losses from Caen stone blocks after 10 RH cycles and initial mass gain on first cycle.

Sample	Mass Loss (% Mass Dry Stone)			Increase in Mass at 1st 70% RH Cycle
	Calcite	Chloride	Nitrate	
1	0.03	0.06	Bd	0.21
2	0.21	0.54	Bd	0.67
3	0.02	0.03	Bd	0.08
4	0.12	0.32	Bd	0.54
5	0.01	0.02	Bd	0.03
6	0.09	0.12	Bd	0.34

Bd below detection, 0.005%.

Significant losses were generated by the 10 cycles of RH. These were not just salt efflorescences, but also calcite from the stone, quantified by mass and identified with FTIR. Only soluble chloride was detected in the losses, no nitrate, despite its presence in the stone. On the first cycle to 70% RH, all the blocks gained mass, presumably due to water vapour sorption. The deliquescent RH of sodium chloride is slightly over 75%; that of sodium nitrate is reported to be above 73%. The water vapour sorption would be unexpected from the reported deliquescent RH value. The measured salt concentrations were inputted into

the ECOS model at 20 °C. The resulting predicted expansions from salt activity are shown in Figure 3.

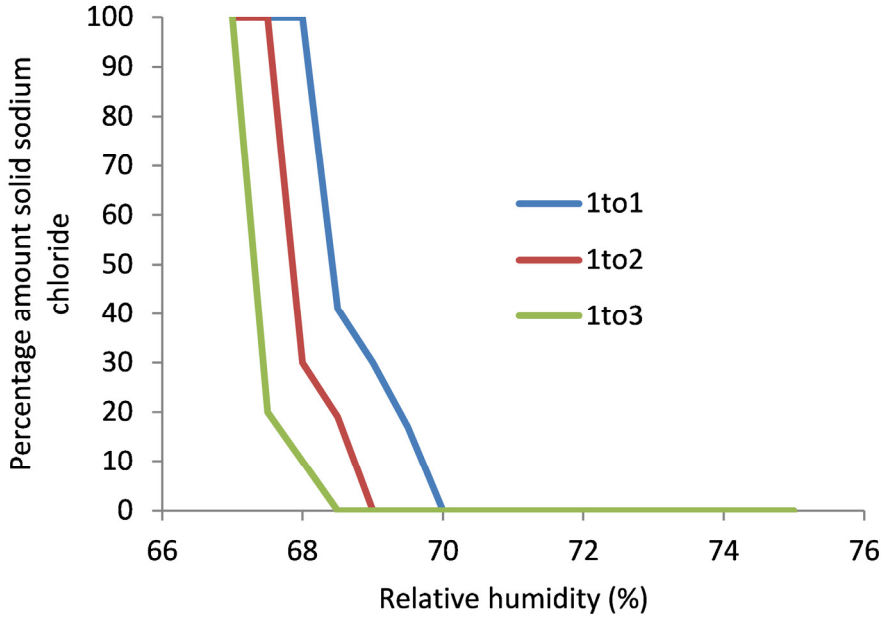

Figure 3. Output from ECOS program for sodium chloride and nitrate mixtures.

As can be seen, the mixtures of sodium chloride and nitrate result in a lowering of the critical RH to 68%, explaining the water sorption at 70% RH and deterioration of the Caen stone surface under the exposure reported.

Total results from the three-year exposure of blocks in the sculpture gallery and store are shown in Table 3.

Table 3. Losses from Caen stone blocks exposed in gallery and store room.

Sample	Mass Loss (% Mass Dry Stone) in Gallery			Mass Loss (% Mass Dry Stone) in Store		
	Calcite	Chloride	Nitrate	Calcite	Chloride	Nitrate
2	0.12	0.25	Bd	0.07	0.18	Bd
4	0.06	0.13	Bd	0.03	0.10	Bd
6	0.07	0.08	Bd	0.04	0.11	Bd

The results follow the same patterns as those reported in Table 2. Higher nitrate ratios increase the amount of damage and no nitrate appears on the surface. These results seem to support the ECOS model outputs. Recent research has provided more data for nitrates [19,20], but this is yet to be parameterised into the model.

Both FTIR-ATR and NIR were found to generate good quality distinctive spectra for kaolinite, palygorskite and sepiolite and could be used for this analysis. The calibrations for the mixes with calcite are shown in Figure 4. The legend includes the wavenumber value of the peak used for calibration. Peaks below 4000 cm^{-1} are FTIR and above are NIR.

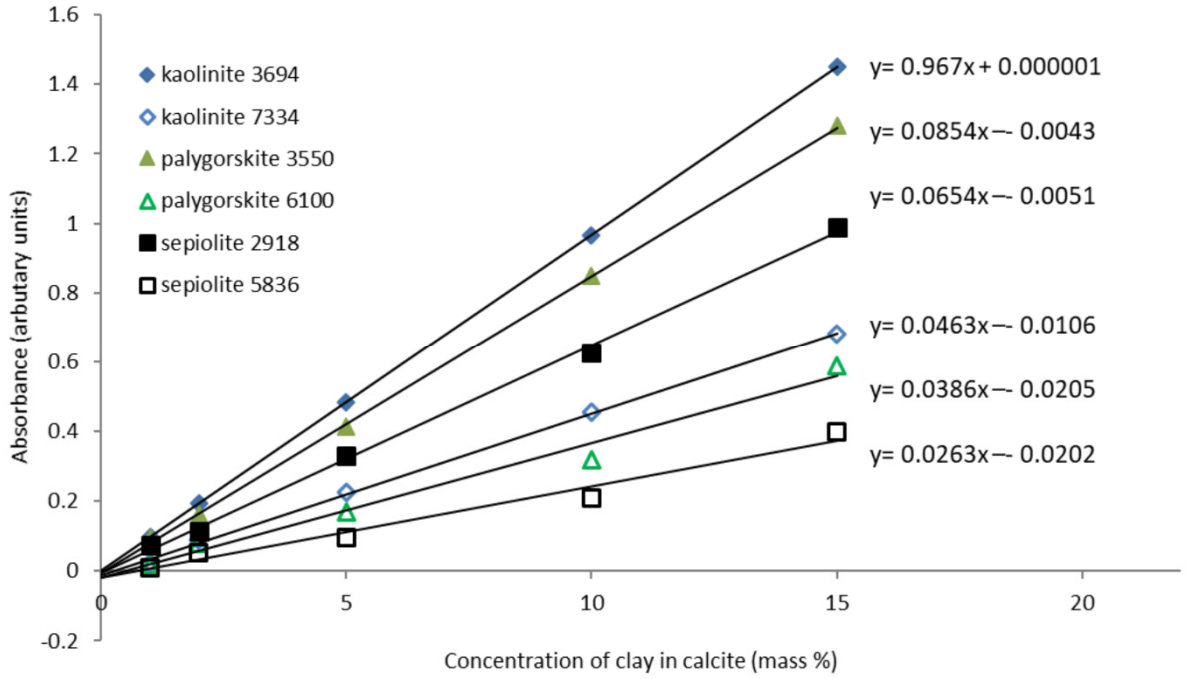

Figure 4. FTIR and NIR calibrations for palygorskite, sepiolite and kaolinite in calcite.

The FTIR calibrations gave better linear fits, were more sensitive and the intercepts were closer to zero. This technique appears more suitable for lower concentrations. At 15%, concentration peaks were significantly broadening and the NIR is perhaps better for higher concentrations. For Egyptian limestones, clay concentrations in the region 2.3 to 19.3% by mass have been measured. The FTIR gave anomalous peak shapes on some analyses, due to dispersion effects. If this was strong, the Kramers-Kroenig correction produced good peak shapes, but for some mixed examples it was not successful. For the standards and 100 stones analysed, good quality spectra could not be produced from approximately 10%. The NIR was able to produce good quality spectra from all samples, although sometimes this required 3 or 4 areas to be analysed.

The depth of calcite from which a signal above the detection limit was detected for each clay/calcite mixture is shown in Figure 5.

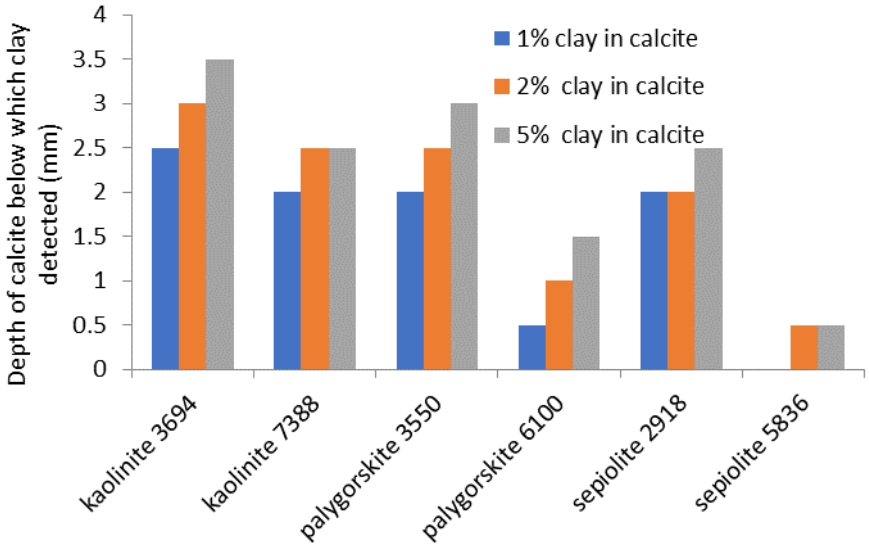

Figure 5. Depth of calcite below with clay mixtures can be detected with FTIR and NIR.

The FTIR detects signals from below greater depths of calcite than NIR. FTIR was shown to be able to detect clays to a minimum depth of 2 mm. For the lowest sepiolite concentration mixture, a depth of 0.5 mm of calcite above the clay blocked the signal, whilst at the occurring 5% concentration, clay signal could be detected below 0.5 mm calcite. These figures are only indications, as factors such as grain size, packing, porosity and water content will affect the radiation transfer through the material. For FTIR, they do indicate that analysis is possible to some depth and for kaolinite and palygorskite with NIR.

Measuring deterioration rate could be used to identify deteriorating limestones and some work has been presented here on quantifying deterioration rates. However, accessible and reproduceable methods are not widely available for this material. Compositional analysis is a faster route to a decision and does not rely on deterioration that may take years to appear to a sufficient degree to be detected.

2.4. Analysing Limestone Composition: Informing Preservation Decisions

Whilst most stone objects are relatively robust and can withstand wide variations in environment, it has been shown that the presence of soluble salts and expanding clays can lead to rapid deterioration. For limestones with predominantly sodium chloride and nitrate present, the critical RH has been assessed and even small excursions above this shown to cause surface damage. The method is readily extendable to any salt mixture using the ECOS thermodynamic model. The presence of some clays, in association with salts, can cause structural damage. FTIR has been shown to be a suitable analysis method to identify the clays in acid insoluble samples more rapidly and with much less sample preparation required than for XRD. Both external reflection FTIR and fibre optic NIR have been shown to allow non-invasive analysis of such clays without any need for drilling. The combined methods allow identification of susceptible limestone objects.

The analysis from the Christ in Majesty sculpture determined chloride concentration of 0.61% (by mass of dry stone), nitrate 0.22% and sodium 0.82%. This similarity to the previously analysed limestones allowed the required climate conditions to be determined. The acid insoluble content was 8.9% kaolinite and this is clearly contributing to the ongoing structural decay. These salt concentrations indicate that maintaining an RH below 68% should retard the deterioration, if not prevent it completely. Attempts at sealing in a polystyrene crate with 3 kg of conditioned Prosorb failed to maintain this RH and deterioration continued. It is planned to move the object into the secure store, which has maintained an RH below 55% for the last decade.

3. Deterioration Rate Measurement

Measuring the deterioration rate of an object in a particular environment can help in making conservation decisions. The yellowing of mastic varnish in nitrogen dioxide containing atmospheres [21] and object silver tarnish rates have been reported [22]. Microfading has become widely used to measure the fading rate of a small spot of a surface, (controlling the colour change to below that visible to the naked eye) [23]. Quantitative rate data can be exceptionally useful for guiding expectations of change and how it manifests. Attempts to use this data to make predictions must consider the many variables within decay processes, as research will record what occurs by fixing variables that may in fact vary in operational environments. Nevertheless, it does provide the only methodology able to contribute to development of predictive decay rates.

3.1. Measuring Deterioration Rates of Archaeological Iron: Introduction

An example of the development of a method for measuring deterioration of individual objects is the application of oxygen depletion as a proxy corrosion rate measurement for complex archaeological iron objects [24–26]. As yet, an incomplete understanding of the decay processes and very complex nature of the objects with many relevant species situated below the surface, has not enabled the compositional analysis approach to accurately predict stability for archaeological iron objects. A body of oxygen depletion results

has been published for archaeological iron that allows interpretation of this data [27–32]. These studies analysed objects from archaeological excavations in England; Battle Abbey, Billingsgate, Camber Castle, Carisbrooke Castle, Carlisle Castle, Chesters Roman Fort, Corbridge Roman City, Dover Castle, Haughmond Abbey, Lullingstone Villa, Pevensey Castle, St Augustine's Abbey, Stonea, Sutton Hoo, Uley, Westminster, Wetwang, Whitby Abbey, Wroxeter Roman City, and one Welsh site, Caerleon.

Based on these oxygen depletion measurements and observations, the collection of iron objects cared for by English Heritage, which is mainly terrestrial archaeology from England, has been found to fall into 4 categories of behaviour Figure 6:

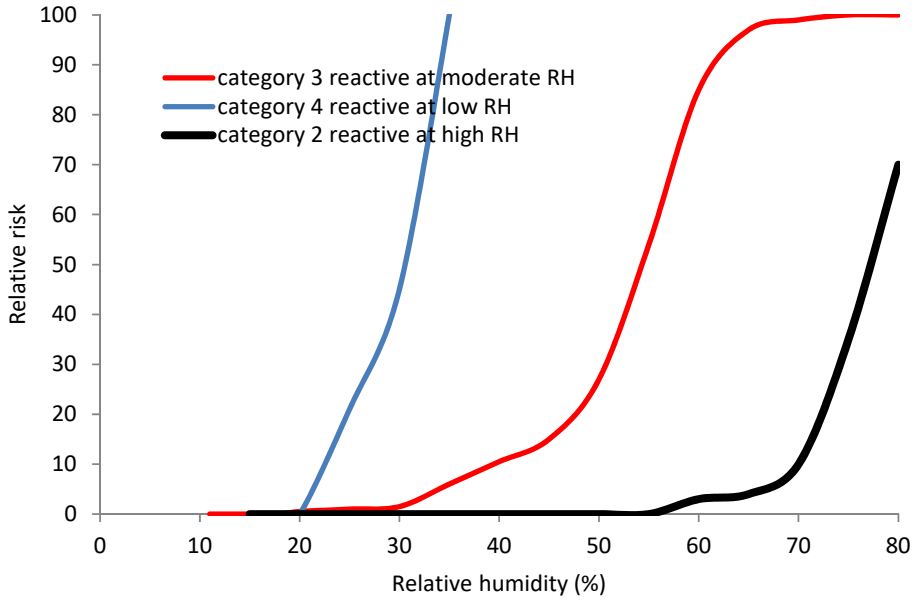

Figure 6. Response of reactive categories of archaeological iron objects to relative humidity. Category 1 has no response.

Response categories are:

1. Material that does not appear to deteriorate even up to very high RH values. Some sites reach 85% RH but no deterioration has been observed visually over 20 years of exposure. These observations are reinforced by oxygen testing of representative samples which show no detectable deterioration at 75% RH. Between 30 and 70% of the archaeological iron in English Heritage collections belongs to this stable group. All sites except Camber had material in this category.
2. Material that deteriorates at higher RH values, with the start point at between 60 and 75% RH. This category included most of the objects from Billingsgate, Haughmond Abbey and Westminster.
3. Material that starts to deteriorate at 11–16% RH. The deterioration rate is quite slow until 30%. It accelerates markedly above 50%. This covers more than 85% of the unstable iron analysed to date and all sites except Billingsgate and Camber Castle.
4. Material that deteriorates slowly at 20% RH, but much more rapidly at 30%. Only three sites have been tested which had objects deteriorating in this way. For two of the three sites, Camber Castle and Stonea all objects underwent this rapid, very low RH deterioration. Not enough objects have been tested from the third site (Carlisle) to confirm this, but visual observation has not determined any signs of deterioration in the remaining iron objects on display.

The results shown in Figure 6 are based on over 900 oxygen depletion measurements and an epidemiological study of over 2800 archaeological iron objects whose response to environments on display and in storage were observed [26,33]. Whilst this is a large number, it is only a small fraction of the English Heritage collection of over 100,000 archaeological

iron objects, hence the large uncertainty reported for the proportion of objects falling into Category 1.

The method of measuring the deterioration rate of iron with oxygen depletion has undergone several improvements over time, which are detailed along with potential limitations for the method [26,34]. With an increasing amount of oxygen depletion data available, this paper seeks to interrogate the distribution of deterioration rates to inform methodological procedures. Any long term changes in deterioration rate over time may prejudice an investigation and it is important that the data reflects the reality of corrosion processes. Tests with copper alloys have shown that if the oxygen concentration drops too low in the reaction vessel or enclosure, this affects the reaction kinetics and therefore the observed rate of corrosion [35]. A potential cause of rate change over time might be if objects crack during oxygen depletion measuring, which could expose the inner material to the environment and speed up the reaction rate. Conversely, if all reactive materials are consumed, then the reactions will cease and oxygen depletion rates drop off. Therefore, understanding the influence of variables in the measurement method on the oxygen depletion rate recorded over time is critical for robust and relevant data collection. Existing data is interrogated here to examine these experimental variables.

3.2. Measuring Deterioration Rates of Archaeological Iron: Method

When the technique was initially adopted for archaeological iron, the method devised involved enclosing the object being tested in either a ground glass stoppered vessel or heat sealed Escal bag, selected so the object mass/container volume was greater than 0.1 g/mL at 50% RH (conditioned with Prosorb) [25]. The oxygen concentration was read with a Gas Sensor Solutions 450 oxygen sensing system from ruthenium complex sensors inside the vessel after 14 days. It was modified with the discovery of the Category 2 response [35], by adding a 3-day exposure period to initially 80% RH, but then the highest RH anticipated, if no oxygen depletion was determined after 14 days at 50% RH. An initial measurement was added at 30% RH on identification of the Category 4 response [27]. Results previously published [26,29,32] using variations of the method were reassessed to investigate the distribution of oxygen depletion rates at 30, 50 and 80% RH across 214 objects and 16 sites.

To investigate the reason for the much lower RH response of the category 4 material, small samples of corrosion were removed and analysed with ATR FTIR (Bruker Alpha) and dynamic vapour sorption, Surface Systems Advantage DVS in zero grade nitrogen. The samples were removed with a scalpel under magnification, targeting the orange crystals previously analysed as akaganeite with Bruker Alpha ATR-FTIR. The samples were analysed with a Thermo IS-10 FTIR with Continuum microscope in direct reflection on a gold coated slide. Only akaganeite was detected with the FTIR microscopy. The technique is insensitive to iron oxides, sulfides and chlorides due to the 650 cm^{-1} cut off of the MCT detector. It is, however, sensitive to iron hydoxyoxides, sulfates, carbonates and phosphates. The DVS recorded the mass of the samples as the relative humidity increased from 5 to 80% RH in 5% RH increments when full mass stabilisation had occurred at each RH. Three samples from a Category 3 site (Dover) were also analysed. The nitrogen atmosphere prevents any oxidation reaction which could cause mass increases that could not be differentiated from those caused by moisture vapour uptake.

Experiments were carried out to investigate the long-term stability of the deterioration rate. Oxygen depletion rate of objects tested in 2005 were re-tested at the same humidity (50% RH) after 13 years. Results from 170 day tests on objects from two archaeological sites were re-examined to compare initial and final oxygen depletion rates.

3.3. Measuring Deterioration Rates of Archaeological Iron: Results and Discussion

The published data for oxygen consumption rates of iron objects is shown in Figures 7–9. The objects are assigned to cohorts corresponding to the category of their corrosion response to humidity, as described above. Cohort 4 objects displayed a Category 4 response, for example.

Different numbers of objects were tested in each cohort and their distributions are shown in 0.2 mbar/year/g bins for 30 and 50% RH and 10 mbar/year/g bins for 80% RH.

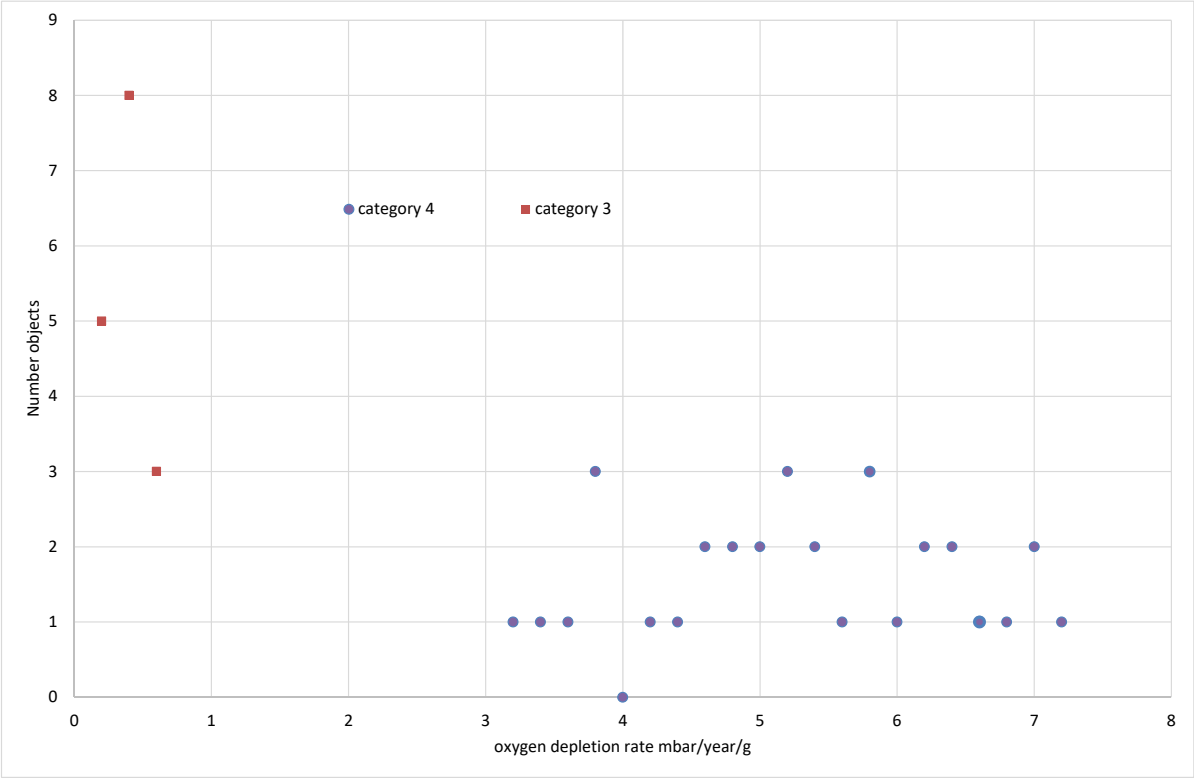

Figure 7. Distribution of oxygen depletion rate at 30% RH for categories 3 and 4.

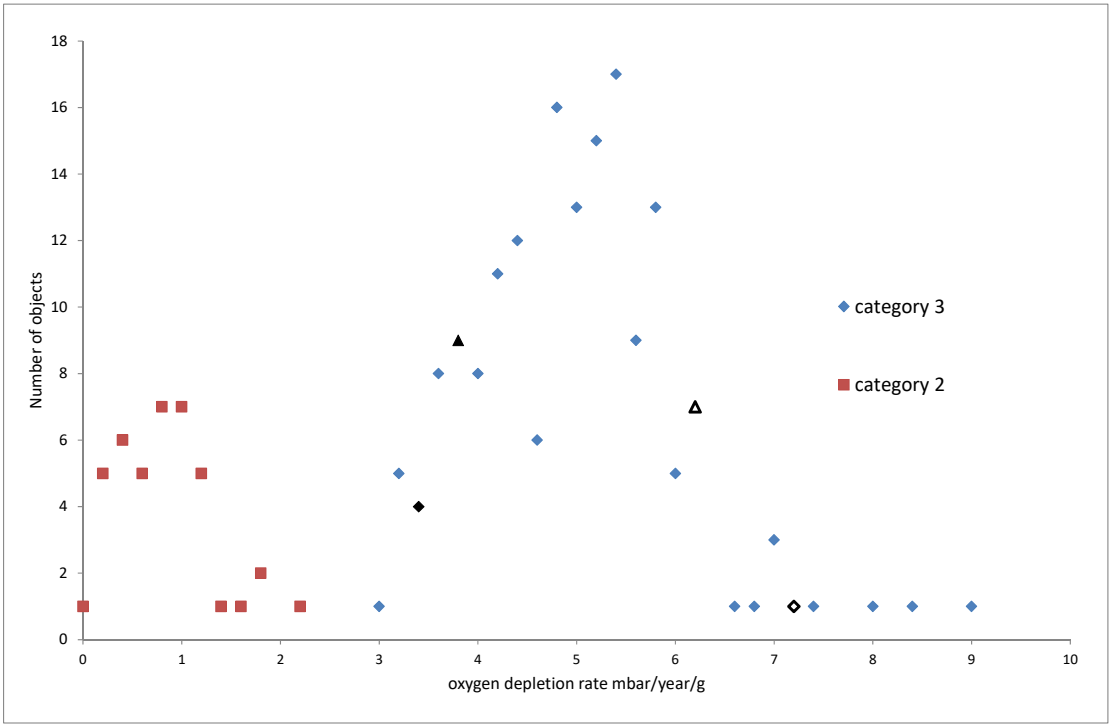

Figure 8. Distribution of oxygen depletion rate at 50% for categories 2 and 3, showing the bins into which 4 objects fell. The four bins into which those objects fell are marked with black hollow and solid diamonds and triangles to differentiate them.

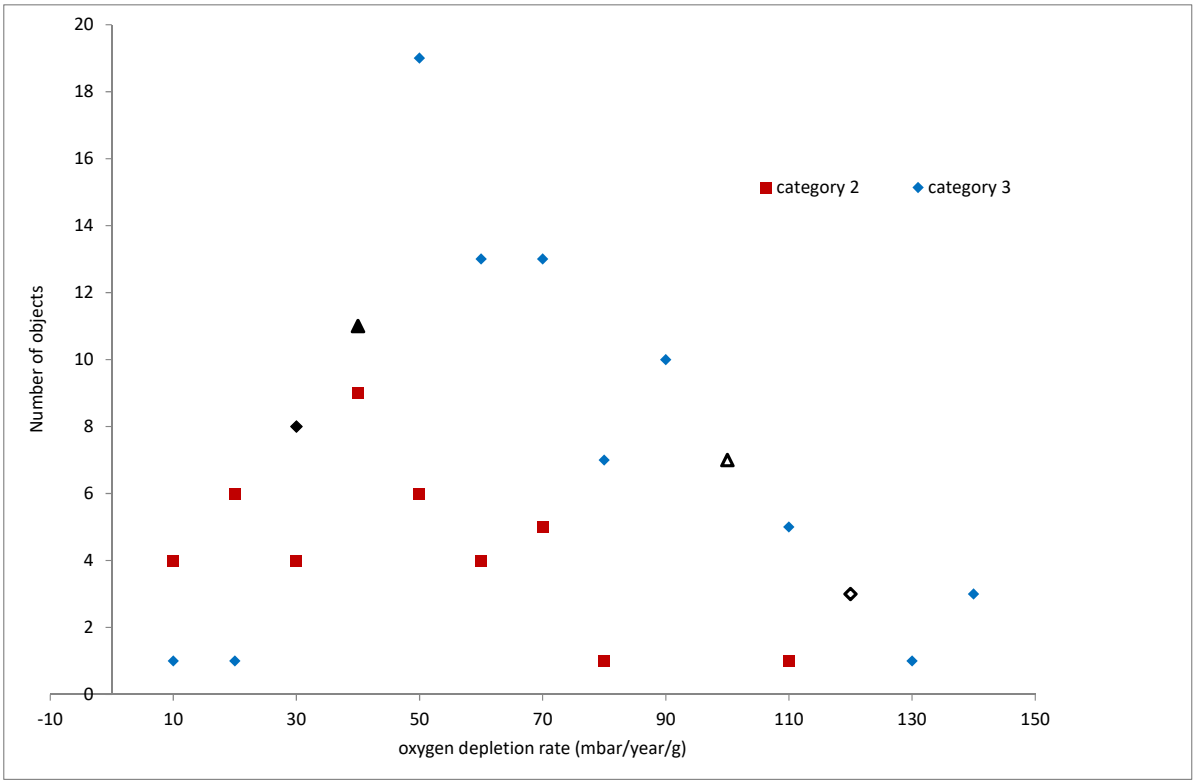

Figure 9. Distribution of oxygen depletion rate at 80% for categories 2 and 3, showing the bins into which 4 objects fell. The four bins into which those objects fell are marked with black hollow and solid diamonds and triangles to differentiate them.

Category 3 reacts much more slowly than category 4 and has a much sharper distribution.

No objects from Category 4 were tested at 50% RH as the reaction rates at 30% were so high. The distributions for categories 2 and 3, are slightly skewed with a few higher reaction rate values.

The reaction rates cover a much wider range of values at 80% RH and the distributions are more skewed. The four individual objects fell within 2 places in the overall ranking of reaction rates compared to the 50% RH tests. This precise measurement of corrosion rate appears to give a good prediction of rates at higher RH values. The measurement overcomes the reliance of averaged rates with large uncertainties for an individual object that is necessary for risk prediction.

The response to increasing RH recorded by DVS for 7 samples of akaganeite corrosion removed from samples from Camber, Carlisle and Dover is shown in Figure 10.

The Dover samples, which lie in Category 3, all showed a slow increase in mass with increasing RH and then a rapid increase above 70% RH. All the Category 4 samples from Camber and the sample from Carlisle showed a rapid increase in mass between 20 and 30% RH.

Table 4 shows the 2006 and 2018 oxygen depletion tests for Lullingstone objects. Between the tests, the objects were kept below either 16% in storage or 30% RH on display.

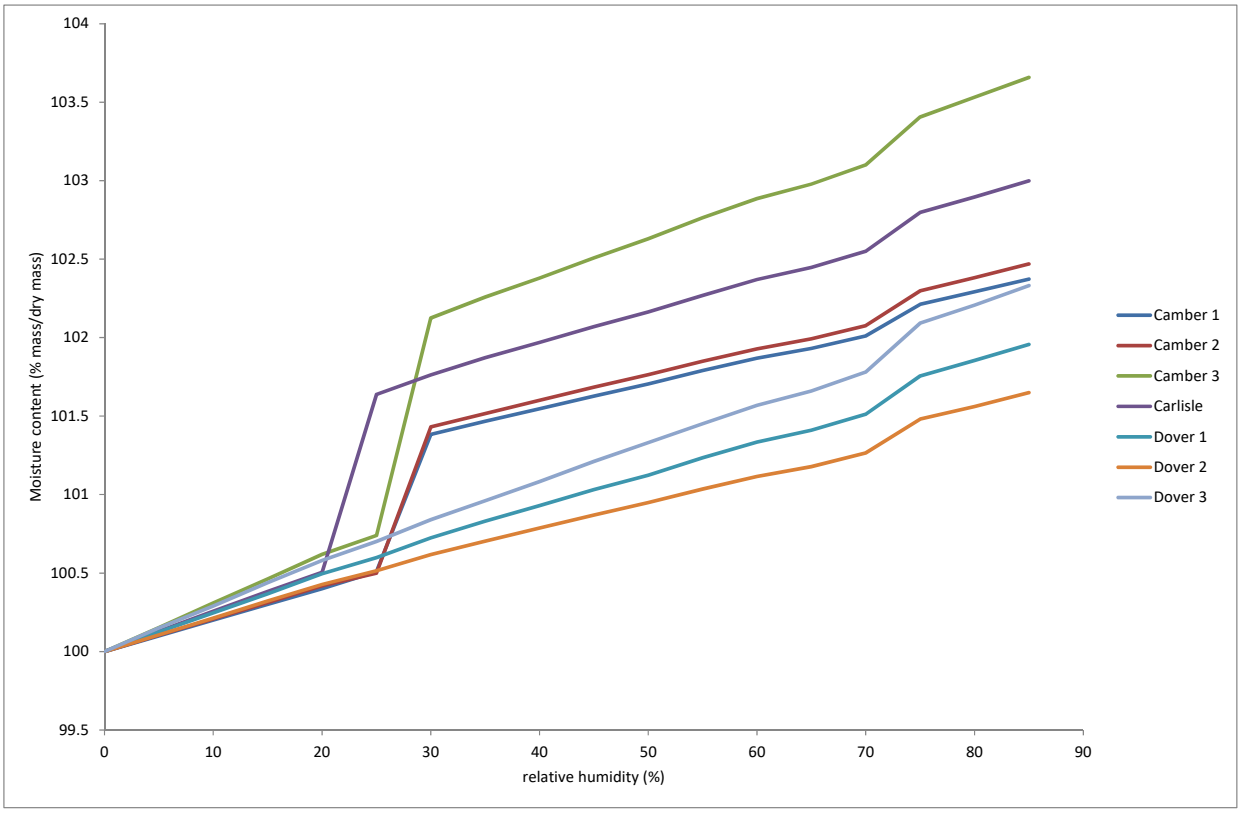

Figure 10. Water vapour sorption results of akaganeite samples from categories 4 and 3.

Table 4. Oxygen depletion values for set of objects in 2006 and 2018.

Oxygen Depletion Rate (mbar/Year/g)		Percentage Change in Depletion Rate (%)
Measured in 2006	**Measured in 2018**	
5.66	5.39	4.8
4.83	4.73	2.1
2.45	2.36	3.5
2.51	2.45	2.4
3.15	3.17	−0.7
3.84	3.78	1.5
2.08	2.12	−2.1
4.49	4.48	0.2
4.34	4.26	1.8
2.32	2.31	0.5
4.14	4.11	0.7
3.49	3.65	−4.5
2.89	2.75	4.8
2.08	2.01	3.6

The values are very similar, within 5% of the initial reaction rate measurement.

The initial and final oxygen depletion rates of objects from sites of Billingsgate and Caerleon during the 170-day tests at 50% RH are shown in Table 5. Rates were calculated over an approximately 14 day period at the beginning (within the first 20 days) and end

(within the final 20 days) of the overall test period. Exact dates vary for each object depending on the measurement schedule.

Table 5. Oxygen depletion values for nails at the beginning and end of exposure to 50% RH for 170 days.

Object	Oxygen Depletion Rate (mbar/Year/g)		Percentage Change in Depletion Rate (%)
	Initial	Final	
1	0.67	0.41	−37.0
2	1.51	0.95	0.8
3	0.98	0.99	−41.9
4	0.40	0.23	6.2
5	0.74	0.79	1.0
6	0.73	0.73	−5.4
7	0.75	0.71	−19.8
8	0.82	0.66	−6.5
9	0.87	0.81	7.8
10	0.93	1.01	19.6
11	0.54	0.65	−23.0
12	2.06	1.59	−2.2
13	0.96	0.94	−13.8
14	0.70	0.60	−9.6
15	5.06	4.57	−1.9
16	3.92	3.85	−4.5
17	4.18	3.99	−1.1
18	15.13	6.37	2.3
19	5.25	5.37	2.9
20	6.00	6.18	0.4
21	5.40	5.43	−3.2
22	4.08	3.96	−31.0
23	3.66	2.52	−22.4
24	3.33	2.59	−22.0
25	8.43	6.58	−4.1
26	3.31	3.17	−3.4
27	4.19	4.05	−6.2
28	3.37	3.17	−37.0
29	0.67	0.41	0.8

There are large differences between the initial and final rates. These tests were completed without opening the vessels, so the oxygen pressure in the tests reduced as reactions progressed. The reactions are likely to be proportional to some function of the oxygen pressure, so the reduced oxygen pressure may influence the result. Almost no enclosures, storage boxes or showcases will be airtight enough for the oxygen not to be replaced by air leakage. Hence, the objects would normally corrode under 20.8% oxygen. Most of the large variations are decreases in the reaction rate. This may indicate over a long exposure at 50% RH, some critical reactants, likely chloride or soluble iron are becoming more limited. Chloride would become bound up in the crystal structure of B-FeOOH if conditions favour

its formation [36], where it could not contribute to corrosion in the short term and this would reduce production of ferrous ions due to oxidation. While corrosion product build up is often cited as reducing corrosion due to limiting access of oxygen and moisture to the metal during corrosion in the atmosphere, this is unlikely to occur for archaeological material as corrosion leads to loss of overlying dense corrosion product layers that already provide this hinderance. There is one exception (19.8%) in the data set with the rate increasing. Otherwise, the increases in rate are of a similar magnitude to the changes measured in Table 4.

Determining that an archaeological iron object reacts in a Category 1 manner, saves resources in drying with silica gel and relaxes showcase design requirements. Many exhibitions also contain mixed archaeological iron or copper alloy with organic materials in the same showcase and some objects comprise mixed materials. The issues that these scenarios raise for managing material-specific and conflicting environmental requirements have been discussed [37]. Identifying Category 1 or 2 iron objects allows a showcase to be developed for the organic material requirements with an understanding that those iron objects are unlikely to be at high risk in these conditions. An added advantage of measuring deterioration rate of iron by oxygen consumption is that an object can be categorised with no requirement to know its chloride content, as the rate is a message to the conservator regarding the stability of the object and hence, the action that must be taken to control corrosion.

3.4. Measuring Deterioration Rates of Archaeological Iron: Informing Preservation Decisions

Previously, environmental limits have had to be set which take into account the range of possible responses of an object type. Examining the oxygen consumption data available for iron objects shows distributions that are very wide and, consequently, very low RHs would be required to stop deterioration in all archaeological iron. As the long term changes in oxygen depletion rate are found to be small or show a decrease in rate with time, this method allows the individual object susceptibility to be assessed. Establishing that an object is not deteriorating at a mid-range RH can offer a significant reduction in resources required to manage environments, with implications for sustainability. It can also significantly reduce the compromise in RH conditions required for mixed display with organic objects. As an approach, it is much more evidence-based and allows a tailoring of conditions to meet individual object needs.

This is exemplified by a cannon ball from Lindisfarne Priory. Oxygen depletion analysis of the cannon ball showed that it did not react at 50% or 60% RH but did at 80%, placing it in Category 2. This permitted its display with bone objects in a showcase conditioned to 40–60% RH with Prosorb. Conversely, a knife blade reacted at 50% RH, indicating Category 3. This prompted a split case design with one portion of the showcase dried with silica gel to between 5 and 30% RH and a separated portion controlled to 40–60% RH with Prosorb for textile objects. Dehumidifiers have been used in mixed display with Category 3 objects. Munters MG50 dehumidifiers have been shown to be capable of maintaining 30–35% RH long term with careful showcase design. Hybrid solutions have also been used with one case containing mixed archaeological iron and organics controlled with a dehumidifier to 30% RH. A second mixed copper alloy and organic case is controlled with silica gel, when this reaches 35% RH, it is swapped with silica gel from the dehumidifier case.

4. State of Preservation

For many materials, degradation processes can cause them to become more environmentally sensitive. Weeping glass develops gel layers that are very sensitive to low RH values [5], whereas glass with thin gel layers shows no low RH sensitivity. As paper degrades, once the degree of polymerisation of the cellulose chains drops below about 300, the paper becomes very sensitive to handling [38]. Research with weighted silk objects indicated a molecular weight below 100,000 Da would require additional support or

conservation to be suitable for display [39]. Light, heat and pollution may cause damage to parchment, as does corrosion of iron gall inks or fading and colour changes to paints. However, in many cases, damage to the text and paint layers is directly related to damage of the parchment structure (e.g., cracking, flaking, etc.). The following example (Section 4.1) examines the role that the state of preservation of parchment can play in its environmental sensitivity and how this influences collections care decisions. An investigation of the application of these principles to leather is also reported (Section 4.2).

4.1. State of Preservation of Parchment: Introduction

Parchment degradation develops from an intact fibre structure of high hydrothermal stability through different stages of fibre structure change that produce decreasing physical and hydrothermal stability. The degradation may progress to a terminal stage with a considerably disintegrated fibre structure that is transformed into a gelatinous substance by contact with water or storage in moist conditions, or into small fibre fragments without any detectable hydrothermal activity.

The IDAP project (Improved Damage Assessment of Parchment) developed methods for characterising the state of preservation of parchment based on shrinkage temperature measurements supported by other advanced analytical techniques [40], including Atomic Force Microscopy (AFM) [41]. The extent of damage was described in terms of 4 major categories according to the state of preservation of parchment, i.e., undamaged, slightly damaged, damaged, heavily to completely damaged, which are shown in Table 6. One of the techniques used in the IDAP project was dynamic mechanical analysis with controlled RH (DMA-RH) [42]. This has also been used recently to study the behaviour of casein films used in food packaging [43]. For parchment, differences in mechanical behaviour with changes in RH were observed for the different damage categories. These differences showed some correlation with differences in shrinkage temperature (Ts). It may be beneficial to vary the environmental conditions in which parchment is stored or displayed according to the extent of its decay, which has been determined and categorised in the IDAP project. This paper proposes, for the first time, the following environmental conditions for each damage category for historical parchment. Further testing of more historical parchment samples is still required to extend the existing database.

Recommendations that come from the IDAP project and which take into account these categories are presented for slightly damaged, damaged and heavily damaged parchment. Parchment in the slightly damaged category is extremely sensitive to changes in relative humidity (RH) and temperature. Even minor variation in these factors may cause changes in its dimensions (area and thickness) resulting in curling and waving of the structure. Moreover, dimensional changes of the parchment may cause damage to text and paint layers. High RH values may accelerate chemical degradation and microbiological attack of the parchment structure. In this damage category it may be expected that a few fibres are damaged to an extent that they may shrink irreversibly at room temperature by exposure to a high RH. Parchment in this damage category should be kept cold under very stable temperature and RH conditions to avoid spontaneous shrinkage or gelatinisation. Only short-term exhibition (e.g., or research purposes) in well regulated and controlled environments should be allowed for parchment. Storage and exhibition conditions should be the same with respect to temperature and relative humidity. For safe keeping of parchment in this damage category it is recommended to make copies of the parchment with text and illuminations for research and exhibition purposes and to take care not to expose the parchment to damaging conditions during the copying. ISO 11799 [44] recommends temperatures between 2–18 °C and RH between 50–60%. However, some micro-organisms thrive at 60% RH, therefore it is recommended to not exceed 45% RH. In mixed collections containing acid papers, it may be especially advisable to maintain an RH of 45% or lower.

Table 6. Proposed damage categories for historical parchment and their recommended environments.

Recommendations for Storage and Exhibition of Parchment in Four Damage Categories					
Category 1-Undamaged-no or very little visible damage, T_f > 43, T_s > 48					
	Max. light (lux)	Max. UV (μW/lumen)	Max. Temp. (°C)	Max. RH (%)	Note
Storage	0	0	18	55	Regularly control
Exhibition	50	75	18	55	Regularly control
Category 2-Slightly damaged—spread minor visible damage (e.g., dirt, stains, some gelatine and/or calcite formation, loss of ink and paint), T_f 30–38, T_s 45–51					
	Max. light (lux)	Max. UV (μW/lumen)	Max. Temp. (°C)	Max. RH (%)	Note
Storage	0	0	18	55	Regularly control
Exhibition	50	75	18	55	Regularly control
Category 3-Damaged—more spread visible damage (some areas may be easy to tear by hand and surface may be partly covered by dirt, stains, some gelatine and/or calcite formation, and suffer from loss of ink and paint), T_f 38–45, T_s 41–49					
	Max. light (lux)	Max. UV (μW/lumen)	Max. Temp. (°C)	Max. RH (%)	Note
Storage	0	0	15	≤45	Regularly control
Exhibition	50	75	15	≤45	Short time exposure
Category 4-Heavily to completely damaged—most part or the whole parchment is very fragile (e.g., felt-like or stiff, brittle and easy to break and the surface may be covered by dirt, stains, severe formation of gelatine and/or calcite and with loss of ink and paint), T_f 29–33, T_s 33–38					
	Max. light (lux)	Max. UV (μW/lumen)	Max. Temp. (°C)	Max. RH (%)	Note
Storage	0	0	≤5	<45	Regularly control
Exhibition	50	<75	2–15	<45	Very short exposure

T_f—first observed shrinkage; T_s—start of the main shrinkage interval.

In the heavily damaged category, fibres may be so damaged that they shrink, gelatinise, melt and/or fragment irreversibly at room temperature on exposure to humidity. Parchment in this damage category should be kept cold or frozen (in case gelatinisation of the parchment takes place below room temperature) under very stable temperature and relative humidity conditions. In some cases, the fibre transformation may even take place at normal RH conditions (50–55%). Exposure to higher temperature, light and electromagnetic radiation will accelerate oxidative reactions leading to degradation of the parchment fibres, binding media, and pigment layers. Higher temperature may also dry out the parchment structure which may cause the parchment to stiffen. Low temperature in combination with a high RH may cause condensation of water on the surface of the parchment. Particular attention should be directed to closed showcases where condensation may occur when the temperature in the surrounding environment drops. This situation may create an ideal microclimate for microorganisms and accelerate chemical reactions.

These general precautions and recommendations are based on the present state of the art knowledge and experience of damage in parchment and the influence of damaging factors in the environment. New knowledge and experiences may therefore lead to detailing or modifications of the recommendations, specifically in relation to research to establish optimum conditions with respect to relative humidity and temperature for storage of parchment in different stages of deterioration. This should include the effect of freezing heavily damaged parchment to stop the process of gelatinising.

Use of the IDAP EWS (Early Warning System) parchment sensor system and data loggers for measurement of RH and temperature is recommended to monitor environmental conditions and warn against potentially damaging factors [40]. In the future, it may be possible to supplement this monitoring with specific sensors for acidic and oxidative pollutants.

The project noted that the recommendations are for guidance only as detailed studies are required to determine which specific climatic conditions provide optimal storage conditions for historical parchment in different degrees of degradation caused by different mechanisms.

4.2. State of Preservation of Parchment: Method

A parchment document (19th century) which was recently acquired (2019) by English Heritage from a private collection, relating to the Wrest Park collection was analysed for its shrinkage temperature (Ts). Several groups of fibres were removed from different (non-text) locations with a scalpel. The fibres were placed in water in a glass slide and heated in a hot stage equipped with a microscope (Mettler FP80, Leitz microscope). The fibres were observed during the heating and the temperature at which the first fibre shrank and then that at which main group of fibres began to shrink noted following the protocol used in the IDAP project.

4.3. State of Preservation of Parchment: Results and Discussion

The fibres from the parchment document had a first observed shrinkage temperature of 48 °C and start of the main shrinkage interval was at 50 °C, placing it in the slightly damaged category according to the IDAP classification. The fibres were considered long, with some splitting and fraying, but no gelatinisation, consistent with the slightly damaged category.

4.4. State of Preservation of Parchment: Informing Preservation Decisions

Using the initial scheme for decision-making in environmental control of parchment, which was based on damage categories developed in the IDAP project (Table 6), guidelines for environmental conditions to match the state of preservation of the document were considered. The example of the English Heritage parchment document in the present study evidences how shrinkage temperature (Ts) measurement and microscopic examination can be used to assign extent of damage for parts of an individual object, where small samples can be taken. The recommended environment for the parchment letter on the basis of Ts (Table 6) is less than 18 °C and 55% RH. In mixed collections containing acid papers, it may be advisable to keep the RH below 45%. International standards developed for all parchments give values of 2–18 °C and 50–60% RH [45]. The more targeted approach was considered superior and adapted. No English Heritage stores are temperature controlled because of object susceptibility (the collection has only a very few pieces of parchment) and for sustainability reasons. Storage was recommended at stores in limestone tunnels under Dover Castle. These naturally maintain temperatures below 18 °C and are dehumidified reliably below 55% RH.

5. Developing Schemes for this Approach

All the approaches discussed require significant knowledge on how materials in increasing states of deterioration react to the environment. The following example shows part of the work required to develop such information.

5.1. State of Preservation of Leather (Vegetable Tanned): Introduction

Leather, like parchment, is a hygroscopic material that reacts very quickly to fluctuations in environmental conditions. The weaker its structure, the less variation in relative humidity and temperature it can tolerate. As with parchment, leather degradation develops from an intact fibre structure of high hydrothermal stability through different stages of fibre structure change that decrease its physical and hydrothermal stability. Measurements of its stability have also been performed by hot stage microscopy. In the STEP project [4] it was concluded that changes in the hydrothermal stability of a given leather are dependent on

the storage conditions and on the tannin type. Hydrolysable tanned leathers are generally more durable than condensed tanned, though the order of durability can change through changes in the storage conditions.

Studies on vegetable tanned leather are reported in this paper to illustrate the work required to build historical leather response databases on which to base environmental recommendations for single objects. Further work will be required to establish an analytical database such as that which already exists for parchment [40].

5.2. State of Preservation of Leather: Method

Leather samples (calfskin) tanned with a mixture of hydrolysable tannins (sumac, valonea and unsweetened chestnut), of thickness 1–1.2 mm split to 0.8 mm, were purchased from the Research Institute of Leather and Plastic Sheeting in Freiberg (Forschungsinstitut für Leder und Kunststoffbahnen (FILK)). Accelerated ageing studies of leather (calf vegetable tanned sumac) were carried out using the methodology reported in the EU funded NANOFORART project (http://www.nanoforart.eu/, accessed on 22 December 2022). The ageing conditions for leather followed the procedure outlined in ISO 5630-5 for paper materials. Samples were aged at 150 °C for 24 h. This provided the opportunity to study changes in the mechanical properties with RH of unaged and aged leather samples. A historical leather sample (calf leather, vegetable tanned) taken from an old book binding (aged approximately 100 years) was also measured. This was provided courtesy of ZFB (Zentrum für Bucherhaltung GmbH, Leipzig https://zfb.com/, accessed on 22 December 2022).

The samples were pre-dried for 24 h and then measured using DMA with controlled RH (See Supplementary Material). Measurements were made in tension under a small strain (0.1%) at 1 Hz using the Dynamic Mechanical Analyser (DMA, Tritec 2000B Lacerta Technology, Loughborough UK) connected to a commercial RH controller. Sample were held in clamps in the DMA and sample size was about 3–5 mms in width and thickness 0.5–0.9 mm with the distance between clamps of 5 mm. Samples were maintained at 20% RH for 30 min and then subjected to a programmed increase in RH (1%/min) to 80% RH. They remained at 80% RH for 100 min and then RH was decreased at 1% RH/min to 30% RH as shown in Figure 10. Changes in displacement expressed as a percentage (D%) of the sample on humidification and dehumidification were recorded with increase in RH (%). This protocol had been used to study parchment in the IDAP project. [40] The calculated values of slope on humidification could then be related to values obtained and used in damage assessment categories for parchment samples in the IDAP project.

5.3. State of Preservation of Leather: Results and Discussion

The resulting displacement (D%) curves plotted against time are shown in Figure 11 for modern and historical samples on humidification and dehumidification. The imposed RH programme is also shown. As the RH increases, the rate of moisture uptake and the accompanying displacement is lower for the historical leather, together with a slower release of moisture on dehumidification.

In Figure 12, the data has been re-plotted against RH. There is a difference in the extent of displacement between the unaged, aged and historical samples with programmed increases in RH. This corresponds with observations for samples of parchment in the IDAP project. There it was demonstrated that the rate of displacement with RH (measured between 20–40% RH) was a marker for the state of preservation of collagen in parchment: i.e., the more damaged (e.g., gelatinised) sample showed very low values of displacement with RH, while relatively undamaged samples showed a much higher displacement [40].

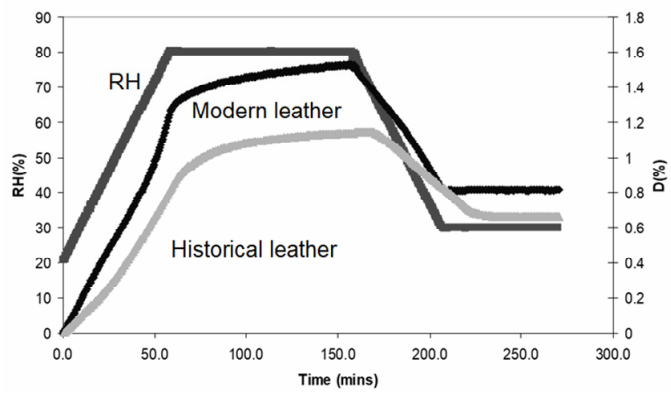

Figure 11. Displacement (D%) of unaged leather sample (black) together with the historical sample (grey) vs. time when exposed to programmed RH (1%/min) (top black curve) from 20 to 80% RH.

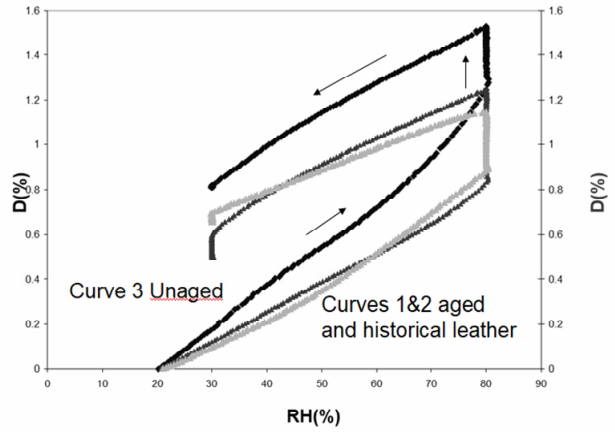

Figure 12. Curves show change in displacement (D%) against RH (%): 1 (grey) and 2 (dark grey) and curve 3 (black) represent aged, historical and unaged leather, respectively. The forward arrow shows the change on humidification, the upward arrow shows the change when the sample remains at 80%RH and the downward arrow shows the change on dehumidification.

Damage to the leather was interpreted in terms of change in D% over RH (20–40%) and compared with values for parchment [40] (Figure 12). The change in slope measured between 20–40% RH for the unaged leather sample showed a higher value (0.019% RH/min) than for the accelerated aged leather sample (0.013% RH/min) (Figure 11). These values interpreted in terms of the IDAP database of DMA-RH for historical parchment samples correspond to categories 3 (damaged) and 4 (heavily damaged), respectively. The historical leather sample gave a value similar to the accelerated aged sample indicating also a high level of damage, i.e., category 4 damage (0.011RH%/min). These categories of damage as established from DMA-RH measurements in IDAP for parchment were found to also correlate with damage as observed using Atomic Force Microscpy (AFM) This non-invasive imaging method (see Supplementary Material) was used in the IDAP project [40] In a subsequent paper [45], it was demonstrated that for thermally aged samples the AFM images showed differing levels of loss of intact collagen surface structure and this correlated both with decrease in shrinkage temperature (Ts) and decrease in rate of displacement with RH when measured by DMA-RH. This correlation opens the opportunity of also using non-invasive AFM for damage assessment. The combination of Ts, AFM, and mechanical testing can provide valuable information on the level of damage incurred by parchment on exposure to environmental fluctuations and pollutants. Recent work [46] has demonstrated that it is possible to image directly on the parchment surface and to observe damaged gelatinised areas close to the text.

Some preliminary measurements using AFM have been made on historical leather samples [47] where its potential to discriminate between the state of preservation of collagen in two different samples was demonstrated: one showed aligned collagen fibrils with characteristic D-banding, and the other showed a complete loss of the collagen banded fibril structure. AFM is used to study collagen structure in biomaterials [47] In addition to AFM, some correlation has also been reported between measurements made using non-invasive technique of unilateral NMR and leather shrinkage temperatures [48].

The leather work is at an initial stage and development is required to validate a reliable analytical methodology and the implications for the environmental requirements of individual leather objects. The leather RH response clearly alters on both accelerated and natural aging. Further work will be required to develop an analytical scheme for leather and more testing is required to validate the parchment scheme for wider application to decision-making.

This general approach of using state of preservation to inform decisions can only be used when suitable analytical methods are available and the results can be interpreted in terms of likely future response to environment. This is not the case for most of the materials comprising cultural heritage at present. However, there have been significant advances in non-invasive, portable analysis over the past two decades [48–50] and several groups are actively working investigating object response [51–53]. The increasing requirements for sustainability and reducing environmental control footprints are likely to drive such work in future.

6. Conclusions

This paper has proposed that, where available understanding, techniques and resources allow, preventive conservation decision-making benefits from being informed by evidence of individual object responses to environments. While broad categorisation of material types can offer a guide to likely appropriate environmental controls, this has a dual disadvantage. It puts at risk any objects whose instability is greater than expected and it is potentially wasteful of resources where objects show no deterioration within a broader range of environmental parameters. As environmental control methods tend to be costly in terms of energy, materials and human resource, a more tailored approach to object needs has the potential to offer more sustainable solutions for storage and display. Sustainability will clearly become even more important within conservation in the coming years and this approach has potential for very significant improvements.

The investigations reported here exemplify the work that is needed to create the knowledge and frameworks required to understand individual object responses within the broader material categories. Three analytical approaches have been proposed and the examples offered evidence how these have been harnessed to understand and modify environmental parameters for objects in the British Museum and English Heritage collections and more widely. The breadth of materials in heritage collections and their variable preservation state presents a great challenge to conservation scientists in developing the frameworks within which to understand individual object responses but the blueprint for doing so, and the advantages this approach offers, are clear.

Supplementary Materials: The following supporting information can be downloaded at: https://www.mdpi.com/article/10.3390/heritage6010011/s1.

Author Contributions: Conceptualization, D.T. and M.O.; Data curation, D.T.; Formal analysis, D.T., N.E., M.O. and D.W.; Investigation, D.T., N.E., R.L. and M.O.; Methodology, D.T., N.E. and R.L.; Resources, N.E.; Writing—original draft, D.T., N.E., R.L., M.O. and D.W.; Writing—review and editing, D.T., N.E., R.L., M.O. and D.W. All authors have read and agreed to the published version of the manuscript.

Funding: This research received no external funding.

Data Availability Statement: All data is available from corresponding author on request.

Conflicts of Interest: The authors declare no conflict of interest.

References

1. ICN. *Limiting Light Damage in Museum Objects: Light Lines*; ICN: Amsterdam, The Netherlands, 2005.
2. *PAS 198:2012*; Specification for Managing Environmental Conditions for Cultural Collections. British Standards Institution: London, UK, 2012. Available online: https://knowledge.bsigroup.com/products/specification-for-managing-environmental-conditions-for-cultural-collections/standard (accessed on 27 July 2022).
3. Watkinson, D. Degree of Mineralization: Its Significance for the Stability and Treatment of Excavated Ironwork. *Stud. Conserv.* **1983**, *28*, 85–90.
4. Larsen, R. *STEP Leather Project, European Commission DG XII, Research Report No. 1*; Larsen, R., Ed.; Bjarnholt Repro: Copenhagen, Denmark, 1994; p. 173.
5. Kunicki-Goldfinger, J.J. Unstable historic glass: Symptoms, causes, mechanisms and conservation. *Stud. Conserv.* **2008**, *53* (Suppl. 2), 47–60. [CrossRef]
6. Tennent, N.; Tate, J.; Cannon, L. The corrosion of lead artifacts in wooden storage cabinets. *SSCR J.* **1993**, *4*, 8–11.
7. Costa, V. The deterioration of silver alloys and some aspects of their conservation. *Stud. Conserv.* **2001**, *46* (Suppl. 1), 18–34. [CrossRef]
8. Newton, R.; Davison, S. *Conservation of Glass*; Butterworths: London, UK, 1989.
9. Letnar, M.C.; Vancina, V.P. The effects of accelerated ageing on graphic paperboards degradation. *Restauro* **2002**, *23*, 118–132. [CrossRef]
10. Bradley, S.M.; Middleton, A.P. A Study of the Deterioration of Egyptian Limestone Sculpture. *J. Am. Inst. Conserv.* **1988**, *27*, 64–86. [CrossRef]
11. Rodriguez-Navarro, C.; Hansen, E.; Sebastian, E.; Ginell, W.S. The Role of Clays in the Decay of Ancient Egyptian Limestone Sculptures. *J. Am. Inst. Conserv.* **1997**, *36*, 151–163. [CrossRef]
12. Price, C. *An Expert Chemical Model for Determining the Environmental Conditions Needed to Prevent Salt Damage in Porous Materials*; European Commission Research Report No 11, (Protection and Conservation of European Cultural Heritage); Archetype Publications: London, UK, 2000.
13. Godts, S.; Orr, S.A.; Desarnaud, J.; Steiger, M.; Wilhelm, K.; De Clercq, H.; Cnudde, V.; De Kock, T. NaCl-related weathering of stone: The importance of kinetics and salt mixtures in environmental risk assessment. *Her. Sci.* **2012**, *9*, 44. [CrossRef]
14. Beatriz, M. Estimation of salt mixture damage on built cultural heritage from environmental conditions using ECOS-RUNSALT model. *J. Cult. Her.* **2017**, *24*, 22–30.
15. Sebastiaan, G.; Roald, H.; De Clercq, H. lnvestigating salt decay of stone materiats related to the environment, a case study in the St. James church in Liège, Belgium. *Stud. Conserv.* **2017**, *62*, 329–342.
16. Godts, S.; Steiger, M.; Orr, S.A.; Stahlbuhk, A.; Desarnaud, J.; De Clercq, H.; Cnudde, V.; De Kock, T. Modeling Salt Behavior with ECOS/RUNSALT: Terminology, Methodology, Limitations, and Solutions. *Heritage* **2022**, *5*, 190. [CrossRef]
17. Środoń, J. Identification and Quantitative Analysis of Clay Minerals. In *Handbook of Clay Science*; Bergaya, F., Benny, K.G.T., Lagaly, G., Eds.; Newnes: London, UK, 2006; pp. 765–787.
18. Bradley, S.M.; Thickett, D. The movement of water and soluble salts in stone. In Proceedings of the Seventh International Conference on the Deterioration and Conservation of Stone, Lisbon, Portugal, 15–18 June 1992; pp. 417–426.
19. Eysseltová, J.; Zbranek, V.; Skripkin, M.Y.; Sawada, K.; Tepavitcharova, S. IUPAC-NIST solubility data series. 89. alkali metal nitrates. part 2. sodium nitrate. *J. Phys. Chem. Ref. Data* **2017**, *46*, 013103. [CrossRef]
20. Gruszkiewicz, M.S.; Palmer, D.A.; Springer, R.D.; Wang, P.; Anderko, A. Phase Behavior of Aqueous Na–K–Mg–Ca–Cl–NO3 Mixtures: Isopiestic Measurements and Thermodynamic Modeling. *J Solut. Chem.* **2007**, *36*, 723–765. [CrossRef]
21. Thickett, D. Measuring object deterioration rates. In *Postprints of Collection Care*; in press.
22. Thickett, D.; Hallett, K. Managing silver tarnish. In Transcending Boundaries: Integrated Approaches to Conservation. In Proceedings of the ICOM-CC 19th Triennial Conference Preprints, Beijing, China, 17–21 May 2021; International Council of Museums: Paris, France, 2021.
23. Ford, B.; Smith, N. A reality check for microfade testing: Five examples. In Proceedings of the ICOM-CC 18th Triennial Conference Preprints, Copenhagen, Denmark, 4–8 September 2017; Bridgland, J., Ed.; art. 1508. International Council of Museums: Paris, France, 2017.
24. Matthiesen, H. A Novel Method to Determine Oxidation Rates of Heritage Materials In Vitro and In Situ. *Stud. Conserv.* **2007**, *52*, 271–280. [CrossRef]
25. Thickett, D.; Lambarth, S.; Wyeth, P. Determining the Stability and Durability of Archaeological Materials. In Proceedings of the 9th International Conference on Nondestructive Testing (NDT) of Art, Jerusalem, Israel, 25–30 May 2008; Available online: www.ndt.net/search/docs.php3?MainSource=65 (accessed on 6 August 2021).
26. Thickett, D. Oxygen depletion testing of metals. *Heritage* **2021**, *4*, 134. [CrossRef]
27. Thickett, D. Post Excavation Changes and Preventive Conservation of Archaeological Iron. Ph.D. Thesis, University of London, London, UK, 2012. Available online: https://www.english-heritage.org.uk/siteassets/home/learn/conservation/collections-advice--guidance/thickettthesisfinalversion.pdf (accessed on 6 August 2021).

28. Thickett, D. The Formation and Transformation of Akaganéite. In Proceedings of the Metal 2013: Interim Meeting of the ICOM-CC Metal Working Group, Edinburgh, UK, 16–20 September 2013; Hyslop, E., Gonzalez, V., Troalen, L., Wilson, L., Eds.; Historic Scotland: Edinburgh, UK, 2013; pp. 103–110.
29. Rimmer, M.; Watkinson, D.; Wang, Q. The Impact of Chloride Desalination on the Corrosion Rate of Archaeological Iron. *Stud. Conserv.* **2013**, *58*, 326–337. [CrossRef]
30. Watkinson, D.; Rimmer, M. Quantifying Effectiveness of Chloride Desalination Treatments for Archaeological Iron Using Oxygen Measurement. In Proceedings of the Metal 2013: Interim Meeting of the ICOM-CC Metal Working Group, Edinburgh, UK, 16–20 September 2013; Hyslop, E., Gonzalez, V., Troalen, L., Wilson, L., Eds.; Historic Scotland: Edinburgh, UK, 2013; pp. 95–102.
31. Watkinson, D.; Emmerson, N.; Seifert, J. Matching Display Relative Humidity to Corrosion Rate: Quantitative Evidence for Marine Cast Iron Cannon Balls. In Proceedings of the Metal 2016: Interim Meeting of the ICOM-CC Metals Working Group, New Delhi, India, 26–30 September 2016; Menon, R., Chemello, C., Pandya, A., Eds.; International Council of Museums Committee for Conservation and Indira Ghandi National Centre for the Arts: New Delhi, India, 2016; pp. 195–202.
32. Watkinson, D.E.; Rimmer, M.B.; Emmerson, N.J. The Influence of Relative Humidity and Intrinsic Chloride on Post-excavation Corrosion Rates of Archaeological Wrought Iron. *Stud. Conserv.* **2019**, *64*, 456–471. [CrossRef]
33. Thickett, D. Using Epidemiology to Validate Scientific Results for Complex Situations. *Metals* 2022, in press.
34. Emmerson, N.J.; Seifert, J.H.; Watkinson, D.E. Refining the use of oxygen consumption as a proxy corrosion rate measure for archaeological and historic iron. *Eur. Phys. J. Plus* **2021**, *135*, 546. [CrossRef]
35. Thickett, D. Critical Relative Humidity Levels and Carbonyl Pollution Concentrations for Archaeological Copper Alloys. In Proceedings of the Metal 2016: Interim Meeting of the ICOM-CC Metals Working Group, New Delhi, India, 26–30 September 2016; Menon, R., Chemello, C., Pandya, A., Eds.; International Council of Museums Committee for Conservation and Indira Ghandi National Centre for the Arts: New Delhi, India, 2016; pp. 180–187.
36. Remazeilles, C.; Refait, P.H. On the Formation of ß-FeOOH (Akaganeite) in Chloride Containing Environments. *Cor. Sci.* **2007**, *49*, 844–857. [CrossRef]
37. Thickett, D. Frontiers of Preventive Conservation, Stud. *Conserv.* **2018**, *63* (Suppl. S1), 262–267. [CrossRef]
38. Thickett, D.; Csefalvayova, L.; Strlic, M. Smart conservation: Targeting controlled environments to improve sustainability. In Proceedings of the 16th Triennial Meeting of ICOM-CC, Lisbon, Portugal, 19–23 September 2011; pp. 19–23.
39. Thickett, D.; Luxford, N.; Lankester, P. Environmental Management Challenges and Strategies in Historic Houses. In Proceedings of the The Artifact, its Context and their Narrative, Getty Conservation Institute, Los Angeles, CA, USA, 6–9 November 2012.
40. Larsen, R. *Introduction to Damage and Damage Assessment of Parchment, Improved Damage Assessment of Parchment (IDAP), Assessment, Data Collection and Sharing of Knowledge*; Research Report no. 18; European Commission: Luxembourg, 2007; pp. 17–21.
41. De Groot, J. Damage Assessment of Parchment with Scanning Probe Microscopy. Ph.D. Thesis, Birkbeck, University of London, London, UK, 2007.
42. Duncan, J.C.; Price, D.M. Thermomechanical, Dynamic Mechanical And Dielectric Methods. In *Principles and Applications of Thermal Analysis*; Wiley: Hoboken, NJ, USA, 2008.
43. Bonnaillie, L.M.; Tomasula, P.M. Application of Humidity-Controlled Dynamic Mechanical Analysis (DMA-RH) to Moisture-Sensitive Edible Casein Films for Use in Food Packaging. *Polymers* **2015**, *7*, 91–114. [CrossRef]
44. *ISO-11799*; Information and Documentation—Documents Storage Requirements for Archive and Library Materials. International Standards Organisation: Geneva, Switzerland, 2003.
45. Odlyha, M.; Bozec, L.; Bartoletti, A.; Melita, L.N.; Larsen, R.; Mühlen Axelsson, K.; Dahlin, E.; Grøntoft, T.; Baglioni, P.; Giorgi, R.; et al. Damage assessment of parchment at the collagen fibril level using atomic force microscopy and mechanical testing at the macro level. In Proceedings of the ICOM-CC 17th Triennial Conference, Melbourne, Australia, 17–19 September 2014; Bridgland, J., Ed.; art. 0607. International Council of Museums: Paris, France, 2014; pp. 73–85.
46. Bartoletti, A. Nanometrology for Damage Assessment and Preservation of Parchment. Ph.D. Thesis, University of London, London, UK, 2017.
47. Odlyha, M.; Bartoletti, A.; Hudziak, S.; Bridarolli, A.; Anders, M.; Thickett, D.; Baglioni, P.; Giorgi, R.; Chelazzi, D.; Bozec, L. A Multi-Analytical Approach to the Characterization of Vegetable-Tanned Leather. In Proceedings of the ICOM-CC 11th Interim Meeting Leather and Related Materials Post-Prints, Paris, France, 6–7 June 2019; International Council of Museums: Paris, France, 2019.
48. Sendre, C.; Badea, E.; Miu, L.; Ignat1, M.; Iovu, H. Unilateral nmr for damage assessment of vegetable tanned leather. correlation with hydrothermal properties. In Proceedings of the ICAMS 2014 5th International Conference on Advanced Materials and Systems, Bucharest, Romania, 23–25 October 2014.
49. Li, Y.; Cheung, C.S.; Kogou, S.; Hogg, A.; Liang, H.; Evans, S. Standoff laser spectroscopy for wall paintings, monuments and architectural interiors. In *Transcending Boundaries: Integrated Approaches to Conservation. Proceedings of the ICOM-CC 19th Triennial Conference, Beijing, China, 17–21 May 2021*; Bridgland, J., Ed.; International Council of Museums: Paris, France, 2021.
50. Wu, W.; Hou, M.; Lv, S. Application of hyperspectral imaging technology to the analysis and research of Chinese paintings and calligraphy. In *Transcending Boundaries: Integrated Approaches to Conservation, Proceedings of the ICOM-CC 19th Triennial Conference, Beijing, China, 17–21 May 2021*; Bridgland, J., Ed.; International Council of Museums: Paris, France, 2021.

51. Kissi, N.; Curran, K.; Vlachou-Mogire, C.; Fearn, T.; McCullough, L. Developing a non-invasive tool to assess the impact of oxidation on the structural integrity of historic wool in Tudor tapestries. *Her. Sci.* **2017**, *5*, 49. [CrossRef]
52. Liu, L.; Gong, D.; Bratasz, L.; Zhu, Z.; Wang, C. Degradation markers and plasticizer loss of cellulose acetate films during ageing. *Pol. Deg. Stab.* **2019**, *168*, 108952. [CrossRef]
53. Pretzel, B. Surface alteration of Japanese lacquers on exposure to (UV-free) light. In *Transcending Boundaries: Integrated Approaches to Conservation. Proceedings of the ICOM-CC 19th Triennial Conference, Beijing, China, 17–21 May 2021*; Bridgland, J., Ed.; International Council of Museums: Paris, France, 2021.